ELSEVIER

Catalysis Today 40 (1998) 215–228

CATALYSIS TODAY

Oxidative dehydrogenation of *n*-butane on MgO-supported vanadium oxide catalysts

J.M. López Nieto[a,*], A. Dejoz[b], M.I. Vazquez[b], W. O'Leary[c], J. Cunningham[c]

[a] *Instituto de Tecnología Química, UPV-CSIC, Avenida de los Naranjos s/n, 46022-Valencia, Spain*
[b] *Departamento de Ingeniería Química, Universidad de Valencia, Dr. Moliner 50, 46100-Burjasot, Spain*
[c] *Department of Chemistry, University College Cork, Cork, Ireland*

Abstract

Vanadium–magnesium oxide (VMgO) catalysts have been prepared, characterized and tested in the ODH of *n*-butane. The catalysts were prepared by two variations of the wet-impregnation method using aqueous ammonium metavanadate or organically-based methanolic vanadyl acetylacetonate solutions. The catalyst surface area depends on the vanadium content and the preparation method. Catalyst characterization (i.e. XRD, ^{51}V NMR, FTIR, LRS) results indicate the presence of poor crystalline Mg-orthovanadate ($Mg_3V_2O_8$), while the presence of other Mg-vanadates is not clear. Oxygen isotopic-exchange experiments on VMgO catalysts indicate an R_2 process: $[^{18}O_2 + 2^{16}O^{2-}_{(s)} \rightarrow (^{18}O^{18}O^{16}O^{16}O)^{4-}_{(s)} \rightarrow 2^{18}O^{2-}_{(s)} + ^{16}O_{2(g)}]$ at temperatures higher than 1023 K, while an R_0-type $[^{18}O_{2(g)} + ^{16}O_{2(g)} \rightarrow 2^{16}O^{18}O_{(g)}]$ is observed at 823 K, as a consequence of a small activity for homophase isotopic. Both the catalytic activity and the selectivity to oxydehydrogenation products depend on the vanadium content but is independent on the catalyst preparation method. This behavior is observed in the ODH of *n*-butane with both O_2 and N_2O. However, while conversion of *n*-butane was higher when using O_2 as oxidant, the selectivity to C_4-olefins was higher with N_2O as oxidant. Pulse experiments show that prereduced surfaces are not effective in producing olefins while selective catalysts are achieved with preoxidized surface. A mechanism for the oxidative dehydrogenation of *n*-butane is proposed. © 1998 Elsevier Science B.V.

1. Introduction

Vanadium–Magnesium oxide (VMgO) catalysts have been proposed as selective catalysts in the oxidative dehydrogenation (ODH) of *n*-butane [1–4] and propane [5–10]. V–Mg–O mixed oxide catalysts have generally been obtained by impregnation of MgO with an ammonium metavanadate solution [1,2,5,11]. However, other preparation methods have been employed, including impregnation of $Mg(OH)_2$ with an ammonium metavanadate solution [6], adsorption of vanadyl compounds from non-aqueous solutions [12,13]; co-precipitation of Mg-nitrate and NH_4VO_3 [14] or of Mg-oxalate and vanadyl oxalate [7,15]; citrate methods [9].

Characterizations of resulting materials have been carried out by several techniques, i.e. XRD [2,3,6,7,9,16], infrared [2,3,6,7,9,11,16], laser Raman [7,9–11,16], diffuse reflectance UV-vis [11,15], ^{51}V NMR [4,6,17–19], EXAFS-XANES [20], TPR [3,4,10,11,21], EPR [21–26], rectangular pulse technique [27], Luminescence [28], XPS [6,7,29,30] and microcalorimetric study of oxygen chemisorption

*Corresponding author. Tel.: 34-6-3877808; fax: 34-6-3877809.

PII S0920-5861(98)00010-8

[27]. The nature of Mg–vanadates revealed by those techniques is found to depend on the V-concentration and the preparative procedure adopted. Dependence on preparative procedure and vanadium content has likewise been reported for the catalytic properties of V–Mg–O catalysts in the ODH of propane, and for the dispersion of vanadium on MgO [7].

Not surprisingly, then, the nature of active and selective sites for the ODH of alkanes is still under discussion. Thus, isolated VO_4 tetrahedra in both amorphous and crystalline $Mg_3V_2O_8$ [1–3,7], dimeric V–O–V-like species on $Mg_2V_2O_7$ [6], or synergetic effects between crystalline phases [9], each have been held mainly responsible for high selectivity in ODH of propane and *n*-butane. Other factors, including the presence of impurities [30,31], the acid–base character of the catalysts [4], or the use of supported vanadium magnesium mixed oxides [32] are also reported to influence the catalytic behavior of these materials.

The aim of the work, reported in the present paper, include further characterization of V–Mg–O catalysts, clarification of the influence of preparative methods on their catalytic properties, and a study of the extent to which activity and selectivity in ODH of *n*-butane could be enhanced by utilizing N_2O rather than using molecular oxygen as oxidant. The extent of agreement of the results obtained in both continuous-flow and pulsed-reactant experiments, with possible mechanisms for the ODH of *n*-butane [2,4,6], is discussed.

2. Experimental

2.1. Catalyst preparation

MgO was prepared by the calcination of magnesium oxalate at 923 K for 3 h. Magnesium oxalate was obtained by precipitation, at pH 5–6, of a magnesium acetate solution with an oxalic acid solution and it was filtered, washed and dried at 353 K for 16 h [7]. Two series of catalysts featuring vanadium supported on such MgO were prepared by two variations of the wet-impregnation method: impregnation with an *aqueous* ammonium metavanadate solution, according to the previously reported procedure [1] (AC-series), or with an organically-based methanolic vanadyl acetylacetonate solution, using different methanol/vanadyl acetylacetonate molar ratio (OR-series) [31]. The solids were dried at 343 K and 27 KPa and then kept at 383 K overnight. Finally, the samples were calcined in air at 873 K for 4 h. Identification of the resulting MgO-supported vanadium catalysts (referred as AC- or OR-series) is afforded by a number that indicates the wt% of vanadium expressed as V_2O_5 (Tables 1 and 2, respectively).

2.2. Catalyst characterization

Chemical analysis of V and Mg was done by atomic absorption.

The BET surface area of the samples, S_{BET}, was obtained in an ASAP 2000 apparatus, from N_2 adsorp-

Table 1
Oxidative dehydrogenation of *n*-butane on V–Mg–O (AC-series) catalysts [a]

Sample	S_{BET} ($m^2\ g^{-1}$)	V-content (wt% V_2O_5)	Temperature (K)	Conversion [b] (%)	Selectivity [c] (%)					
					1-B	2-t-B	2-c-B	BD	CO	CO_2
13-AC	145	12.8	773	23.6	12.4	4.3	5.1	15.2	13.9	47.8
			823	48.8	7.5	2.3	2.7	24.4	16.0	45.9
19-AC	108	18.8	773	22.0	16.0	5.9	7.3	22.6	11.8	34.9
			823	43.0	10.9	3.3	4.0	31.8	13.7	34.9
40-AC	68.1	39.6	773	15.9	17.6	7.4.	8.7	18.0	10.6	36.0
			823	33.7	13.7	4.5	5.5	27.0	12.8	34.9

[a] The catalytic tests were carried out at a contact time, *W*/*F*, of 10.1 g_{cat} h(mol-C_4)$^{-1}$.
[b] Conversion of *n*-butane.
[c] Selectivity to 1-butene (1-B), 2-trans-butene (2-t-B), 2-cis-butene (2-c-B), butadiene (BD), and carbon oxides (CO and CO_2). Other products as propene and ethene were detected as traces.

Table 2
Oxidative dehydrogenation of *n*-butane on V–Mg–O (OR-series) catalysts [a]

Sample	S_{BET} ($m^2\ g^{-1}$)	V-content (wt% V_2O_5)	Temperature (K)	Conversion [b] (%)	Selectivity [c] (%)					
					1-B	2-t-B	2-c-B	BD	CO	CO_2
8-OR	66.8	7.9	773	11.6	17.5	7.3	8.7	10.4	11.1	42.7
			823	28.3	14.5	4.9	6.0	22.8	12.8	36.7
18-OR	46.5	18.4	773	11.0	21.9	9.7	12.1	16.6	8.8	28.6
			823	24.4	18.2	6.7	8.5	26.8	10.2	27.8
36-OR	44.0	35.6	773	19.1	18.2	8.1	9.7	20.0	11.2	31.4
			823	40.6	12.6	4.3	5.4	27.9	16.8	32.6

[a] The catalytic tests were carried out at a contact time, *W/F*, of 10.1 $g_{cat}\ h(mol\text{-}C_4)^{-1}$.
[b] Conversion of *n*-butane.
[c] Selectivity to 1-butene (1-B), 2-trans-butene (2-t-B), 2-cis-butene (2-c-B), butadiene (BD), and carbon oxides (CO and CO_2). Other products as propene and ethene were detected as traces.

tion isotherms at 77 K and taking a value of 0.164 nm^2 for the cross-section of N_2.

X-ray diffraction (XRD) patterns were collected in a Philips 1060 diffractometer, equipped with graphite monochromator, operating at 40 KV and 40 mA and using nickel-filtered CuK_α radiation (λ=0.1542 nm).

Solid-state ^{51}V NMR spectra were recorded at ambient temperature on a Varian VXR-400S WB spectrometer at 105.1 MHz, using a high speed MAS Doty probe with zirconia rotors (5 mm in diameter). The spectra were recorded with pulses of 1 μs corresponding to a flip angle of $\pi/13$, in order to avoid signal distortions of the I=7/2 nuclei. To obtain the MAS–NMR spectra, samples were spun at 7 KHz. The ^{51}V chemical shifts are referenced against liquid $VOCl_3$, using a 0.16 M $NaVO_3$ aqueous solution, whose chemical shift is −574.3 ppm, as a secondary reference.

The infrared spectra were recorded at room temperature on a NICOLET 710 FTIR spectrometer equipped with Data Station. Dried samples of 20 mg each were mixed with 100 mg of dry KBr and pressed into a disk (600 kg cm^{-2}).

Laser Raman spectra (LRS) were recorded with an FT-Raman spectrometer (Bio-Rad, Model RAMAN-II) incorporating an Nd : YAG laser (Spectra Physics, Model FC-106C-10). About 400 scans were co-added to produce each spectrum. The optimum power was selected as a compromise between signal and sample heating effect.

Temperature-programmed reduction (TPR) results were obtained in a Micromeritics apparatus. Samples of 10 mg were first treated in argon at room temperature during 1 h. The samples were subsequently contacted with an H_2/Ar mixture (H_2/Ar molar ratio of 0.15 and a total flow of 50 ml min^{-1}) and heated, at a rate of 10 K min^{-1}, to a final temperature of 1173 K.

Experiments to assess the influence of vanadium oxidation state on N_2O decomposition were made using a temperature-programmed reaction technique, TPR_x-N_2O. This involved, firstly, establishing of a steady flow of N_2O (diluted in He such that $P_{N_2O} = 140$ torr) over a preoxidized or prereduced catalyst aliquot at room temperature allied to suitable sampling arrangements for mass spectrometric monitoring of exit gas composition. The temperature was then ramped at 10 K min^{-1} and profiles vs. temperature were obtained for exit gas composition, i.e. N_2O, O_2 and N_2.

2.3. Catalytic tests

2.3.1. Continuous flow experiments in conventional reactor

These were carried out in a fixed bed, stainless-steel tubular reactor (i.d. 20 mm; length 520 mm). A coaxially centered thermocouple was used, which could be moved up and down along the catalyst bed for temperature profiling. The catalyst charge was 0.2–0.5 g (particle size 0.30–0.50 mm) mixed with 8 g of Norton

silicon carbide (particle size 0.50–0.75 mm) to obtain a constant volume in the catalyst bed. Different contact times (W/F=2–40 g_{cat} h $mol_{C_4}^{-1}$), were used in order to obtain different *n*-butane conversion levels. The feed consisted of *n*-butane, oxygen or N_2O, and helium in a molar ratio of 5 : 20 : 75 ($C_4 : O_2 : He$) or 5 : 40 : 55 ($C_4 : N_2O : He$), with a total flow of 100 to 600 cm^3 min^{-1}. The catalytic tests were conducted at atmospheric pressure in the 773 to 823 K temperature interval. Analysis of reactants and products were carried out by gas chromatography using two columns: (i) Carvosieve-So (8 m×1/8") and (ii) 23%SP-1700 Chromosorb PAW (30 m×1/8").

Specific activities (in mol_{C_4} h^{-1} m^{-2}) and turnover (in mol_{C_4} h^{-1}/mol-V) were calculated, from data achieved at 773 K and conversions of *n*-butane (X_t) lower than 10%, considering the following equations:

$$\text{specific activity} = \frac{X_t}{W/F \times S_{BET} \times 100} \quad (1)$$

$$\text{turnover} = \frac{X_t \times 50.9}{W_v/F \times 100} \quad (2)$$

where W_v is the amount of vanadium of catalyst (in g) tested.

Blank runs showed that under the experimental conditions used in this work the homogeneous reaction can be neglected. In all cases, the lowest total flow used was 100 ml min^{-1}.

2.3.2. *Pulsed reactant experiments in microreactors*

Comparisons between initial activities of the catalysts for *n*-butane conversion in unsteady-state condition were made by passing individual micropulses of *n*-butane, (typically 0.45 μmol), alone or admixed with O_2 (70 torr) or N_2O (140 torr), in an argon carrier gas over small catalyst samples (∼10–40 mg) at W/F=14 to 56 g_{cat} h $mol_{C_4}^{-1}$ and T_{rx} from 773 to 823 K. On-line GC analysis of each exit pulse was achieved on a 30 m×1/8" 23% SP-l700 chromosorb PAW column. Tests with the empty reactor indicated insignificant homogeneous gas phase conversions of *n*-butane in these conditions.

2.3.3. *Oxygen isotope exchange at catalyst surfaces*

An entropically non-equilibrated (l.n.eq.) mixture, having ca. 50% of each $^{18}O_2$ and $^{16}O_2$, was used as a gas phase probe, whose isotopic composition can serve as a versatile and sensitive indicator for the occurrence of R_0-, R_1-, or R_2-type oxygen isotope exchange processes on oxide surfaces [34]. Tests for such processes over aliquots of V/MgO samples were made in an all-glass recirculatory reactor system equipped with MS to monitor isotopic composition of the recirculating oxygen gas at 30 s intervals. The normal in-situ pretreatment sequence given to catalysts prior to introduction of the ($^{16}O_2$+$^{18}O_2$) mixture comprised: (i) heating to 823 K while $^{16}O_2$ was recirculated over the sample and through a trap at 77 K to eliminate H_2O; (ii) cooling to room temperature (RT) in the $^{16}O_2$; and (iii) evacuation at RT to remove it. Following introduction of the ($^{18}O_2$+$^{16}O_2$) mixture at ca. 5 mbar, onset temperatures for oxygen isotope exchange processes over such preoxidized samples were first identified from profiles of temperature-programmed oxygen isotope exchange (TPOIX) carried out at 30 s intervals, while temperature was ramped at 10 K min^{-1}. Such TPOIX profiles indicated that the onset of heterophase oxygen isotope exchange processes did not become apparent in such experiments until temperatures much higher than 773–823 K range (of direct relevance to ODH activity of the materials) were attained. In an effort to evaluate even very slow oxygen isotope exchange over the preoxidized samples at 773 or 823 K as catalytically interesting temperatures, other experiments were carried out with the same recirculatory reactor system and fresh aliquots of ($^{18}O_2$+$^{16}O_2$), but isothermally and with long-term monitoring of the isotopic composition of the recirculating gas.

3. Results and discussion

3.1. *Catalyst characterizations*

Data in Tables 1 and 2 show that the overall BET surface decreased with increasing vanadium content in both the AC-series and OR-series.

Powder XRD patterns of the V-containing samples confirmed the coexistence of crystalline MgO, with peaks at 2θ=42.97 and 62.48 (JCPDS 4-829), together with poorly crystalline Mg-orthovanadate, $Mg_3V_2O_8$ phase, with peaks about 2θ=35.0 (JCPDS 19-779). For samples in the OR series, crystallinities of

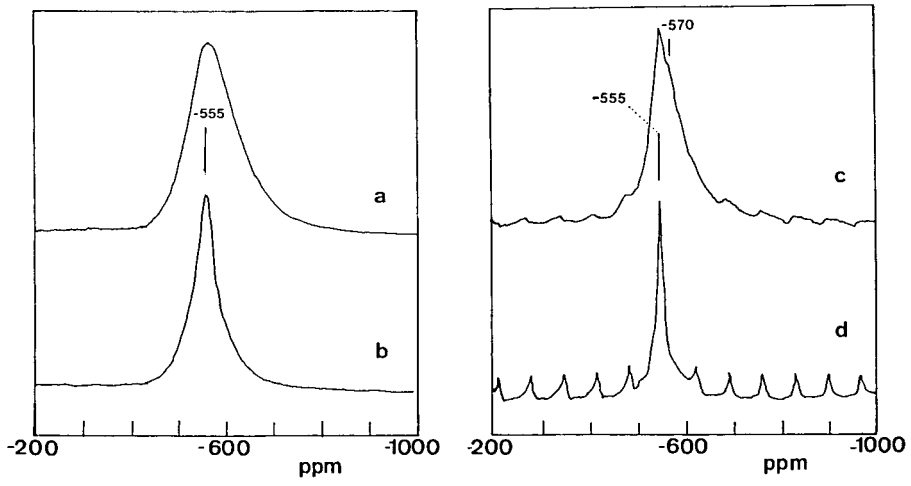

Fig. 1. ^{51}V wideline (a, b) and MAS–NMR (c, d) spectra of MgO-supported vanadium oxide catalysts: 19-AC (a, c); 18-OR (b, d).

the latter appeared to increase to a greater extent with vanadium content, than for samples in the AC-series.

Fig. 1(a) and (b) clearly show the ^{51}V wideline spectra of catalysts with only one band centered at −555 ppm. This band appears broader in catalysts with low vanadium loading and prepared by aqueous method (13-AC and 19-AC samples). The fact that other bands in the 250–450 ppm interval are not observed in the wideline spectra indicates that only tetrahedral V^{5+} species are present at significant concentrations on the as-stored catalysts [4,6,17–19].

In addition, the MAS–NMR spectra of samples 19-AC and 18-OR are shown in Fig. 1(c) and (d), respectively. In the first case (Fig. 1(c)), two bands at −554 and −570 ppm are observed while in the spectrum of sample 18-OR (Fig. 1(d)) only a band at −570 ppm can be seen. According to previous results [4], the band at −554 ppm originates from vanadium in a crystalline $Mg_3V_2O_8$ phase while the band at −570 ppm could be related to distorted VO_4 tetrahedron units which are highly dispersed on the MgO surface.

In the infrared spectra of all the catalysts studied here, the most intense band appeared at 426 and 860 cm^{-1}. The first band is related to the presence of MgO. However, the appearance of the bands of low intensity at 965, 917, 849, 687, 550 cm^{-1}, in addition to band at 860 cm^{-1}, on catalysts with high vanadium loading indicates the presence of $Mg_3V_2O_8$, in agreement with previous results [2,3,6,7,9,11,16]. Despite the detection of a weak feature at 965 cm^{-1}, suggestive of the presence of other Mg-vanadates, the recent literature raises another possibility. Thus, the presence of a band at 965 cm^{-1} in the IR spectra, formerly attributed to $Mg_2V_2O_7$ [3,6,11], has recently been proposed to originate from highly dispersed and probably of low crystallinity $Mg_3V_2O_8$ on the MgO surface [9].

Laser Raman (LR) spectra of MgO-supported vanadium oxide catalysts (AC-series) are shown in Fig. 2. Only a broad band centered at 880 cm^{-1} is observed on the 13-AC sample, which decreases with increasing vanadium loading. Conversely, two bands at 860 and 830 cm^{-1} increase with the vanadium loading of catalysts, and can be attributed to the increased presence of crystalline $Mg_3V_2O_8$ [7,9–11,16]. A generalization proposed in relation to LR spectra is that the higher the symmetry of tetrahedral vanadium species the lower the wave number at which its LR bands appear [33]. On that basis, the broad band centered at 880 cm^{-1}, here observed on samples prepared in an aqueous medium and having low vanadium content, could be due to the presence of non-crystalline distorted V^{5+} species with a tetrahedral coordination and/or to the presence of polymeric (VO_3) or dimeric V–O–V species. However, ^{51}V-NMR spectra confirm that associated V-species were not formed at any of the vanadium loadings studied here. Thus it can be proposed that species responsible for the LR feature at

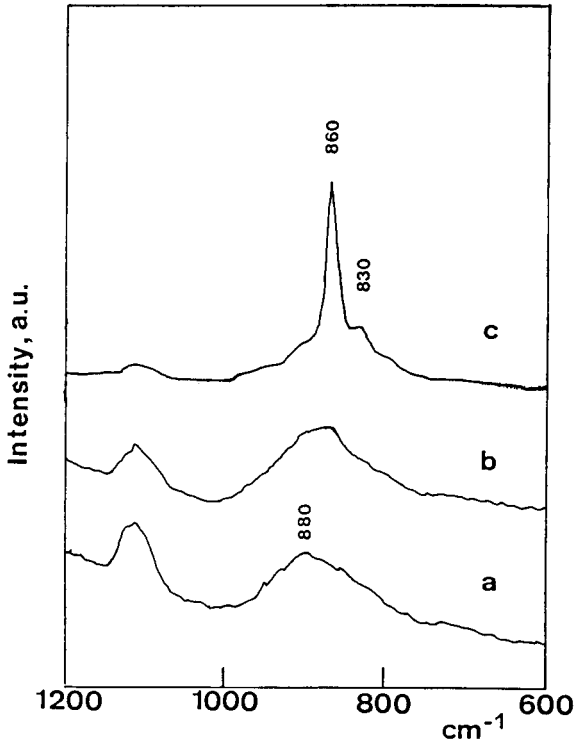

Fig. 2. Laser Raman spectra of MgO-supported vanadium oxide catalysts: (a) 13-AC, (b) 19-AC, and (c) 40-AC.

880 cm^{-1} correspond to distorted VO_4 tetrahedra which is highly dispersed on the surface of MgO at low loadings.

TPR profile showed two peaks at ca. 633 and 833 K on catalysts with low vanadium loading prepared by either method. On the other hand, V^{5+} species of low reducibility as indicated by a single TPR peak (at 833 K) were mainly observed in OR-series catalysts with vanadium loading higher than 10 wt%. However, a single peak at 923 K was observed on sample 39-AC. Similar results were observed previously on mixed VMgO catalysts [3] and two types of vanadium species, in which the most readily reducible ones are mainly formed on catalysts with low vanadium content, were proposed. Such differences in detail, between the TPR profiles of AC-series and OR-series samples, reinforce the indications provided by LR and IR that changes in wet-impregnation preparative procedures can significantly alter the relative amounts of dispersed vanadia subsets, differing in degree of distortion and in redox properties.

3.2. Results of oxygen isotope exchange and N_2O dissociation by mass spectrometry

Fig. 3 presents the results of experiments carried out with ca. 5 mbar of ($^{18}O_2$+$^{16}O_2$) in contact with Vanadia/MgO catalyst samples in a recirculatory reactor system. This features a liquid-N_2 cooled trap as part of the recirculatory loop in order to ensure negligible residual pressures of H_2O or CO_2 which otherwise could promote isotopic exchange with $^{18}O_2$ [35]. The objective of the experiments was to discover whether the vanadia/MgO materials would evidence activity for heterophase oxygen isotope exchange processes as per Eq. (3) and Eq. (4).

$$R_1\text{-type}: {}^{18}O_{2(g)} + {}^{16}O^{2-}_{(s)} \rightarrow ({}^{18}O{}^{18}O{}^{16}O)^{2-}_{(s)} \rightarrow {}^{18}O_{(s)}{}^{2-} + {}^{16}O{}^{18}O_{(g)} \quad (3)$$

$$R_2\text{-type}: {}^{18}O_{2(g)} + 2{}^{16}O^{2-}_{(s)} \rightarrow ({}^{18}O{}^{18}O{}^{16}O{}^{16}O)^{4-}_{(s)} \rightarrow 2{}^{18}O^{2-}_{(s)} + {}^{16}O_{2(g)} \quad (4a)$$

$${}^{18}O_{2(g)} + ({}^{16}O^{-}\text{–}{}^{16}O^{-})_{(s)} \rightarrow {}^{16}O_{2(g)} + ({}^{18}O^{-}\text{–}{}^{18}O^{-})_{(s)} \quad (4b)$$

MS monitoring of the isotopic composition of the recirculating gas phase, while temperature of the V/MgO sample was ramped upward at 10 K min^{-1}, yielded the TPOIX results shown in Fig. 3(a) when a preoxidized vanadia/MgO sample was used, and those in Fig. 3(b) over a prereduced sample. Fig. 3(a) makes clear that onset of heterophase oxygen isotope exchange did not occur until temperatures higher than 1023 K, i.e. ca. 473 K above those at which such catalysts could be of interest to promote ODH of butanes.

Fig. 3(a) illustrates that the predominant net effects of oxygen isotope exchange, observed in the preoxidized sample, would remove $^{18}O_{2(g)}$ from the gas phase and its replacement by $^{16}O_{2(g)}$ will be supplied in some way by $^{16}O^{n-}$ species of the metal oxide. Then term 'place exchange' has sometimes been employed to categorise processes with these net effects [36] especially in the absence of significant production of $^{16}O^{18}O_{(g)}$. The latter is seen to be the case in Fig. 3(a), which demonstrates that R_1-type isotopic exchange via Eq. (3) remained insignificant up to high temperatures in the TPOIX run. Conversely, the observed predominance of place exchange could be

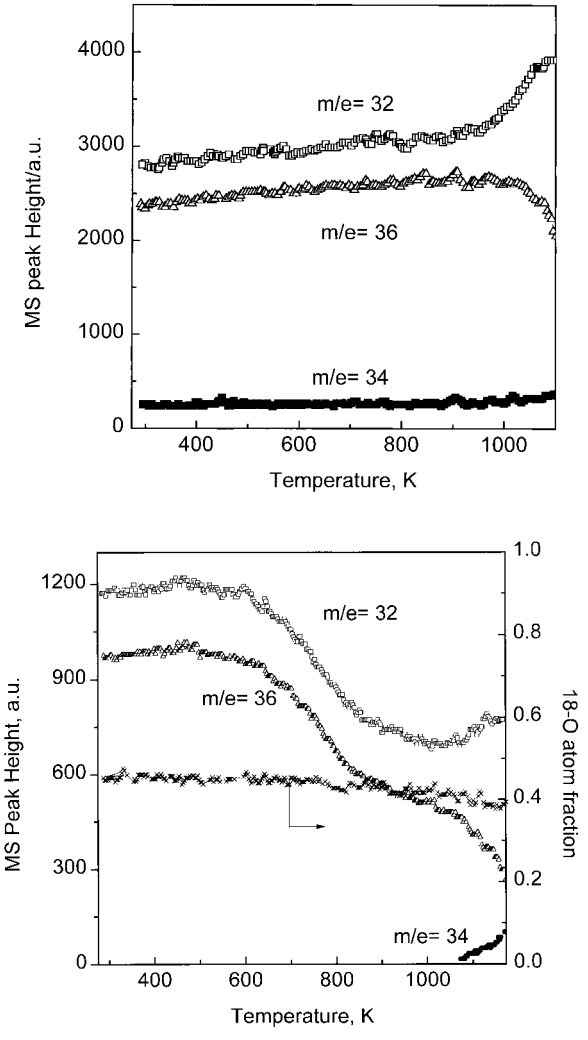

Fig. 3. Variation of the partial pressures (arbitrary units) of $^{18}O_2$ (*m/e*=36), $^{16}O^{18}O$ (*m/e*=34) and $^{16}O_2$ (*m/e*=32) in the gas phase over 500 mg of 18-OR sample in a recirculatory reactor: (a) over the preoxidised sample during temperature ramp of 10 K min^{-1}; (b) over the same sample under same ramp, but with sample prereduced 1 h in H_2 at 823 K and outgassed prior to admitting 5 mbar of ($^{16}O_2$+$^{18}O_2$). Data points on the horizontal plot correspond to the invariant atom fraction of ^{18}O in the gas phase (as per vertical scale on r.h.s.).

accounted for Eqs. (4a) and (4b), involving diatomic oxygen exchange between $^{18}O_2$ and adjacent pairs of $^{16}O^{2-}_{(s)}$, or between $^{18}O_2$ and peroxy-type $(^{16}O^{-}–^{16}O^{-})_{(s)}$ on the surface of V/MgO at high temperatures.

The results obtained from a similar TPOIX experiment over a prereduced aliquot of the same material (cf. Fig. 3(b)) show an expected additional feature, namely the uptake of $^{18}O_2$ and $^{16}O_2$ from the 5 mbar dioxygen gas phase, due to reoxidation of the prereduced vanadia/MgO catalyst by the dioxygen species, with onset temperature of ca. 625 K. It is clear not only from the parallel slow declines of *m/e*=36 and 32 at ramp temperatures 625 to 750 K, but also from the invariant value for the atom fraction of ^{18}O in the gas phase (line a.f in the plot), that reoxidation was not accompanied by significant R_1- or R_2-type heterophase oxygen isotope exchange processes at those temperatures. Again it is only at temperatures higher than 1023 K that there is evidence for onset of place-exchange type oxygen isotope exchange consistent with Eq. (4a) or Eq. (4b).

Fig. 4 presents results from long-term isothermal monitoring of the isotopic composition of the dioxygen gas phase following contact at 823 K between 5 mbar of the ($^{18}O_2$+$^{16}O_2$) gaseous probe with a preoxidised aliquot of the 18-OR sample. The invariant value of ca. 0.45 for the ^{18}O atom-fraction in the gas phase throughout the 250 min contact between dioxygen and the 18-OR sample at 823 K demonstrates the absence of any detectable heterophase oxygen isotope exchange via Eq. (3) or Eq. (4). How-

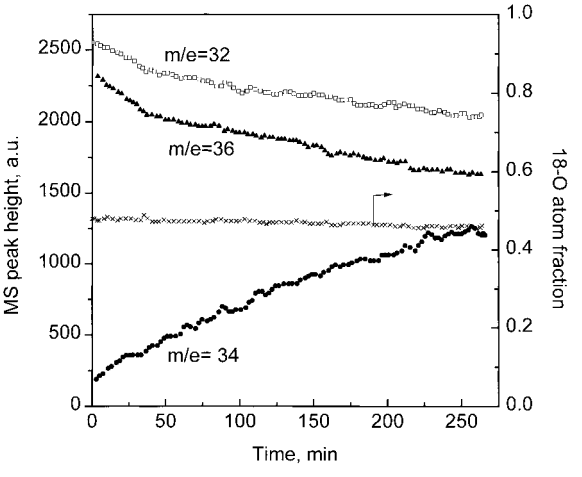

Fig. 4. Variation of the partial pressures (arbitrary units) of $^{18}O_2$ (*m/e*=36), $^{16}O^{18}O$ (*m/e*=34) and $^{16}O_2$ (*m/e*=32) in the gas phase over 500 mg of 18-OR with duration of contact with ($^{16}O_2$+$^{18}O_2$) in isothermal conditions at 823 K over the preoxidised sample. Data points on the horizontal plot correspond to the invariant atom fraction of ^{18}O in the gas phase (as per vertical scale on r.h.s.).

ever, the slow parallel decline, seen for m/e=36 and 32, with a converse rise in m/e=34, show that the sample did exhibit, at 823 K, some small activity for homophase isotopic equilibration of the gas phase in accordance with Eq. (5), which occurs without the lattice oxygen-16 species, leaving the surface and entering the gas phase:

$$R_0\text{-type}: {}^{18}O_{2(g)} + {}^{16}O_{2(g)} \rightarrow 2\,{}^{16}O{}^{18}O \quad (5)$$

A promoting effect of dispersed VO_4 tetrahedra by loss of one oxygen, on such events would be in line with previous proposals that activity for such R_0-type isotopic equilibration requires composite metal oxide sites featuring both a coordinatively unsaturated cation of variable valency and an anion vacancy capable of localising an electron at a shallow trapping level [37].

The successful use of nitrous oxide as an alternative gaseous oxidant to dioxygen in promoting ODH of butane over vanadia/MgO (vide infra) is of interest in determining the temperature profile for N_2O decomposition (TPR_x) over the catalyst when preoxidized or prereduced. Determination of such profiles by an experimental procedure, allowing only brief contact between N_2O and the catalyst, was appropriate, since such brief contacts would later feature in pulsed-reactant catalytic experiments involving passage of (n-butane+N_2O) pulses over the same materials. Relevant (TPR_x) profiles for dissociation of N_2O (140 torr in helium) over 18.4% V_2O_5/MgO were obtained by on-line MS analysis of the exit gases from continuous flow at W/F=14.8 g h $mol^{-1}_{N_2O}$ under temperature ramp of 10 K min^{-1}. The profiles obtained over the preoxidized 18-OR sample made it clear that only relatively small extents of N_2O dissociation ranging from 15 to 30% at T_{rx} 773–823 K resulted and that reasonable mass balance existed between decrease in N_2O and growth of N_2+1/2O_2 product. Even slower rates for decrease of P_{N_2O}, and for converse increases in P_{O_2} and P_{N_2} were found in an equivalent TPR_x-N_2O experiment over a sample of this 18-OR material prereduced at 873 K.

3.3. *Catalytic oxidative dehydrogenation of n-butane with O_2 or N_2O under continuous flow*

Tables 1 and 2 show the catalytic behavior of V_2O_5/MgO catalysts prepared in aqueous or methanolic media, respectively. In all cases, C_4-olefins (1-butene, 2-tras-butene, 2-cis-butene and butadiene), CO and CO_2 were the only reaction products with 20% O_2 as co-reactant. It should be noted that in all the catalysts studied here, selectivities to oxydehydrogenation products higher than 50% were obtained at butane conversions lower than 40%.

Fig. 5 shows the specific activities (calculated at 773 K and n-butane conversions lower than 10%) and the corresponding turnover of the catalysts. A tendency of specific activity to increase with V-loading is evident with 36-OR rather than 40-AC. In respect of turnover, the 36-OR sample is also exceptional in being somewhat higher than for the 40-AC sample of comparable V-loading. At lower V-loading of ca. 18%, the reverse is true with less turnover for 18-OR than for 19-AC. However, within either the OR-series or AC-series, the highest turnover was observed for the lowest V-loading studied. This trend for turnover to decrease with increasing V-loading points to a decreasing number of ODH sites with increasing V-loading. Since, present characterizations of the materials indicated higher crystallinities at higher loadings and for OR-series, the trend of turnover values in Fig. 5 is consistent with an inverse relationship between crystallinity and turnover.

Variation of the selectivity to the main reaction products as a function of the butane conversion on the 19-AC sample at 773 and 823 K is shown in Fig. 6.

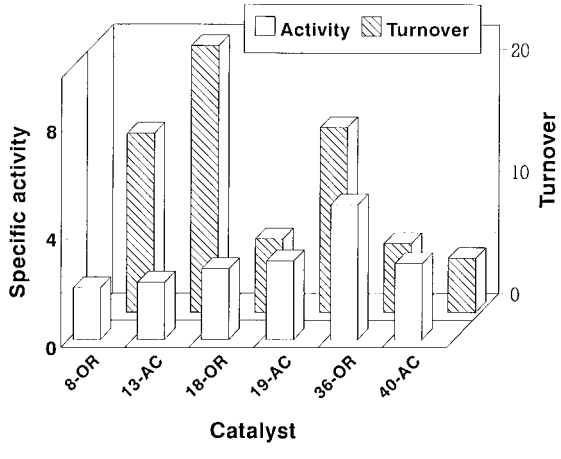

Fig. 5. Variation of the specific activity (in mol-C_4 h^{-1} m^{-2}) and the turnover (in mol-C_4 h^{-1}/mol-V) with the catalyst vanadium content of MgO-supported vanadium oxide catalysts. Reactions conditions: T=773 K; n-butane conversion lower than 10%.

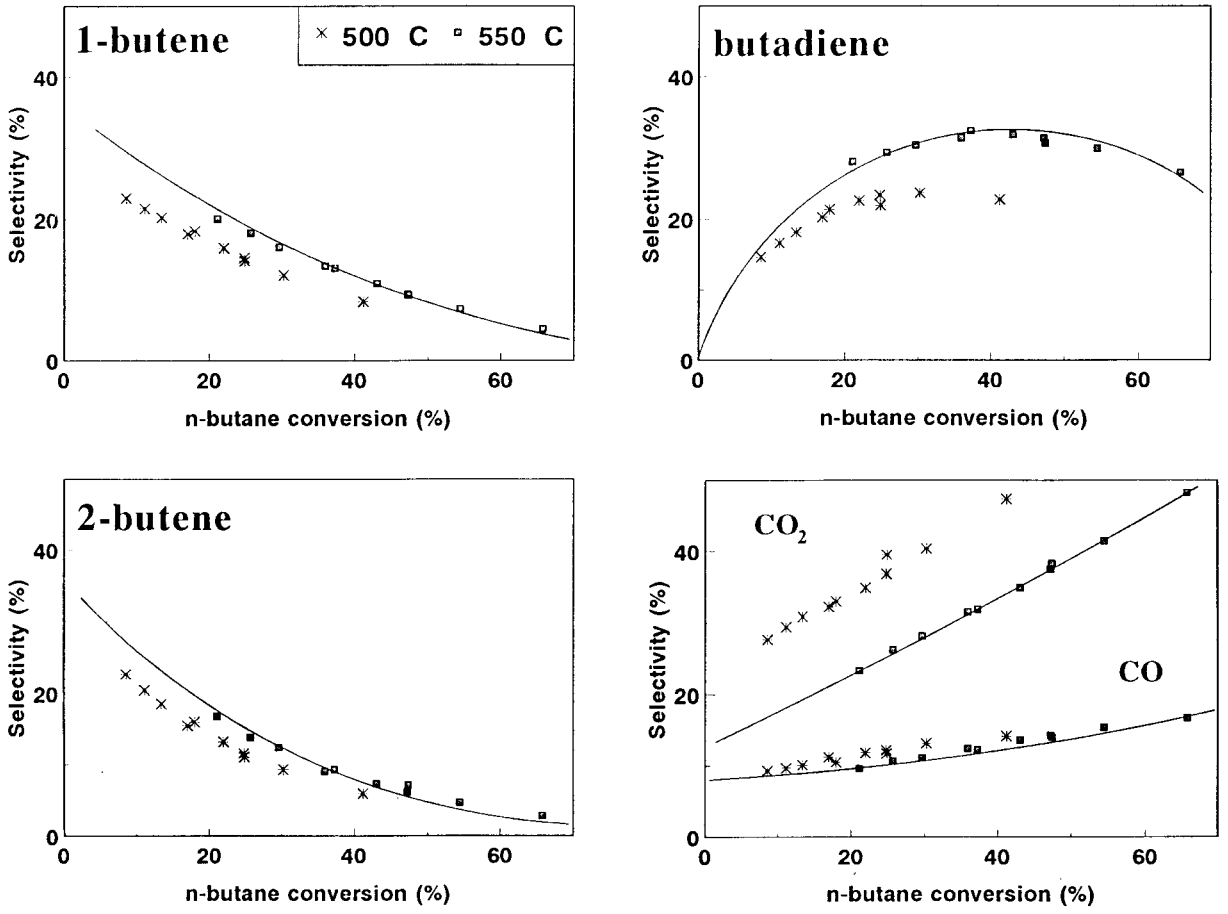

Fig. 6. Variation of the selectivities to 1-butene (1-B), 2-butenes (2-B), butadiene (BD), CO and CO_2 with the conversion of *n*-butane on the 19-AC sample at a reaction temperature of 773 and 823 K.

Similar results were obtained on the other samples. The selectivity to monoolefins decreases with the butane conversion, while the selectivity to butadiene initially increases with the butane conversion, showing a maximum at butane conversion of 40%. On the other hand, CO and CO_2 are formed at low butane conversion (with initial selectivities of ca. 20–30%) and their selectivities increase as the butane conversion is increased. In addition, it can be seen that the selectivity to C_4-olefins increases with the reaction temperature while the selectivity to CO_2 shows an opposite trend.

Fig. 7 shows variation of the selectivity to each C_4-olefin with the vanadium content (as V_2O_5). It can be seen that samples with vanadium loading higher than 15 wt% are the most selective catalysts. However, small differences in the selectivity to C_4-olefins are observed on these samples.

Scheme 1 represents a possible reaction network for the oxydehydrogenation of *n*-butane, which is broadly consistent with the foregoing results using dioxygen as oxidant. Formation of a butyl radical via hydrogen abstraction from butane by surface lattice oxygen is envisaged, followed by loss of a second hydrogen to yield monoolefins, butadiene formation by consecutive reactions, and competition due to carbon oxide formation from both butyl radicals and butenes [2,4].

Prompted by literature reports on the use of N_2O as oxidant in catalysis of alkane ODH by other metal-oxide-supported catalysts [38–42], such studies were

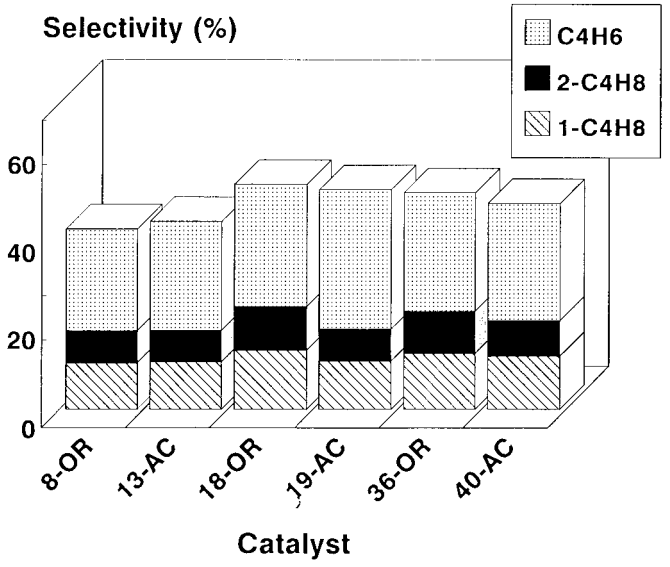

Fig. 7. Variation of the selectivity to each C_4-olefin over the various catalysts with their vanadium contents (comparison mode at a *n*-butane conversion of 10% and a reaction temperature of 773 K).

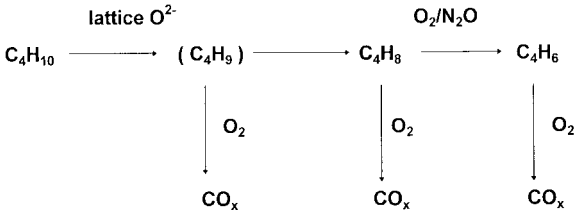

Scheme 1. Reaction network for the oxidative dehydrogenation of *n*-butane with O_2 or N_2O as co-reactant.

made using a continuous flow of (C_4H_{10}+N_2O) as feed gas in order to establish the extent to which N_2O as oxidant affected steady-state catalytic performance of the MgO-supported vanadium oxide catalysts. Data comparing the catalytic behavior of OR-18 sample during the ODH of *n*-butane using O_2 or N_2O as oxidant are summarised in Table 3. Data shown therein for the same temperature and identical contact time, show that the conversion of *n*-butane with O_2 as oxidant was higher than with N_2O, whereas the selectivity to oxydehydrogenation products was higher when N_2O was used as oxidant. The observation of lower overall *n*-butane conversion with N_2O as oxidant rather than O_2 – despite equal oxygen-atom content in the feed gas in both cases – implied that N_2O induces decreases in a rate-limiting step of Scheme 1. On the other hand, although comparisons between selectivities to butadiene achieved at 773 and 823 K under similar *W/F* values show higher selectivities at 823 K with either O_2 or N_2O as oxidant, proportionately greater enhancement is achieved with N_2O. An important contributory factor to such enhancement by N_2O at 823 K appeared to be significantly greater diminution of selectivity to CO_x for the C_4H_{10}/N_2O system at that temperature (cf. data at *W/F*=20.1 in Table 3). Present data do not permit unequivocal conclusions to be drawn concerning possible contribution to those differences by processes similar to those identified by other workers for (alkane+N_2O) reactant over other vanadium containing solids: (i) proposals by Bellussi et al. [38] that formation of O^- species from N_2O were responsible for higher selectivity to propene and onset of propane conversion at lower temperatures over vanadium silicalite than with O_2 as oxidant; and (ii) proposals by Ilchenko et al. [41] that a higher activation energy for methane oxidation by O_2 than by N_2O was responsible for greater alkane oxidation with N_2O than O_2 at 723 K, but the converse at 823 K.

3.4. Pulse experiments

Realistic objectives of pulsed-reactant experiments, involving a succession of brief, low-exposure contacts

Table 3
Oxidative dehydrogenation of *n*-butane on the 18-OR sample using O_2 or N_2O as oxidant

Contact time, *W*/*F*	Conversion [a] (%)	Yield [b] (%)	Selectivity [c] (%)					
			1-B	t-2-B	c-2-B	BD	C_2–C_3	CO_x
C_4H_{10} : O_2 : He=5 : 20 : 75 (*T*=773 K)								
10.1	11.0	6.7	21.9	9.7	12.1	16.6	1.1	37.5
20.1	17.0	9.3	18.4	7.4	9.4	19.3	1.1	43.8
39.3	24.9	11.5	14.1	5.3	6.7	20.0	1.1	52.3
C_4H_{10} : O_2 : He=5 : 20 : 75 (*T*=823 K)								
10.1	24.4	14.7	18.2	6.7	8.5	26.8	1.4	38.0
13.5	29.1	16.6	16.0	5.8	7.7	27.5	1.4	41.3
20.1	35.4	18.1	13.3	4.4	5.7	27.8	1.4	47.2
C_4H_{10} : N_2O : He=5 : 40 : 55 (*T*=773 K)								
16.4	4.6	3.6	27.3	16	18.2	17.8	2.3	16.6
32.8	7.1	5.4	23.8	12.8	14.6	23.8	4.1	20.8
65.6	12.5	9.2	17.4	9.6	11.0	35.7	2.8	23.6
C_4H_{10} : N_2O : He=5 : 40 : 55 (*T*=823 K)								
10.9	11.2	8.5	23.5	11.1	13.5	27.7	5.6	18.6
32.8	23.0	16.0	14.4	8.3	7.4	39.6	4.7	25.7
65.6	30.4	18.6	10.2	4.4	4.7	41.9	4.4	34.4

[a] Conversion of *n*-butane at 823 K.
[b] Yield of C_4-olefins in %.
[c] Selectivity to 1-butene (1-B), 2-trans-butene (2-t-B), 2-cis-butene (2-c-B), butadiene (BD), propene and ethene (C_2–C_3) and carbon oxides, CO and CO_2 (CO_x).

between gaseous reactant(s) and Vanadia/MgO catalysts of the types described here, included the following:

(i) Tests of the validity, for present catalysts, of the central importance of lattice oxygens in allowing such catalysts to initially achieve initial activities and alkene selectivities in ODH of alkane, even in the absence of any gaseous oxygen. Confirmation of this point is provided by the data summarized in bar-chart form within Fig. 8(A). Part A of the figure shows overall conversions of the *n*-butane content of alkane-only pulses at 773, 798 and 823 K, and corresponding overall selectivities to C_4-olefins on contact of pulses with preoxidized 25 mg aliquots of catalyst (sample 18-OR). Those observations may be contrasted with results from pulsed-flow catalytic experiments over aliquots of the catalyst which had been severely pre-reduced in flowing H_2 at 973 K prior to introduction of butane-only pulses. Those are summarized in bar-chart form in Fig. 8(B) and evidence an order-of-magnitude decrease in butane conversions relative to those at corresponding temperatures over non-pre-reduced aliquots (cf. Fig. 8(A)), thus making it clear that ready availability of surface lattice oxygens on 18.4% V_2O_5/MgO strongly promoted *n*-butane activation in initial pulses at 773, 798 and 823 K. Another, and somewhat more surprising, negative effect on the initial, non-steady-state activity of this catalyst was found on switching from delivery of four butane-only pulses at 803 K over the preoxidized catalyst to delivery of four pulses having 67 torr of O_2, premixed with the butane and then switching back to butane-only pulses. No measurable selectivity toward butadiene was found from any of the 'butane plus premixed O_2' pulses, in striking contrast to the observation of butadiene selectivities in the range of 20±10% from the preceding or subsequent butane-only pulses. Rationalization of that limited data is possible in terms of autocatalytic generation of some ODH-active sites by butane-only pulses, but with development of such sites being averted due to rapid reoxidation by the oxygen content of (butane+O_2) pulses.

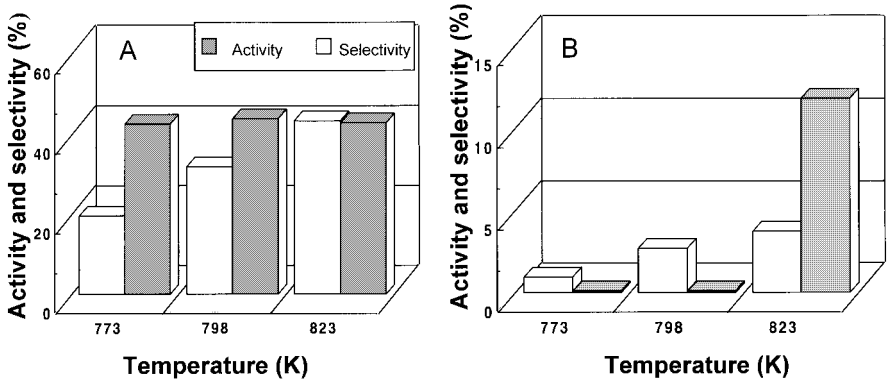

Fig. 8. Comparison of the initial, non-steady-state activity of 25 mg of 18-OR sample in converting 14 torr pulses of butane-only at 773, 798 and 823 K, and of accompanying olefin selectivity. (A) Sample preoxidised and then outgassed before commencing pulse sequence; (B) Sample prereduced in H_2 at 973 K and out-gassed before pulse sequence.

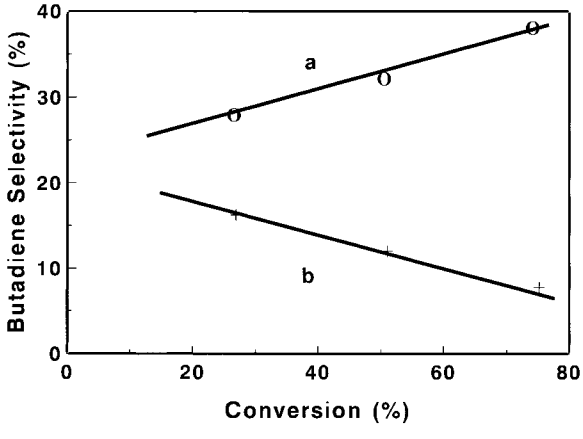

Fig. 9. Variation of the selectivity to butadiene with the conversion of *n*-butane for pulses over preoxidised 18-OR catalyst. (a) with $P_{N_2O} = 140$ torr and P_{butane}=14.8 torr; (b) with $P_{O_2} = 70$ torr and P_{butane}=15.0 torr.

(ii) Over aliquots of catalyst (sample 18-OR) having ready availability of surface lattice oxygens (i.e. in preoxidized form), a *comparison* was made as to how the ratio (Percentage C_4-alkene product selectivity): (Percentage *n*-butane conversion) varied when N_2O replaced O_2 as gaseous oxidant admixed with *n*-butane in reactant pulses. A higher ratio of $N_2O : C_4H_{10}$ than that of $O_2 : C_4H_{10}$ (9.5 and 4.8, respectively) was used to ensure comparable at% oxygen content in the reactant. The two plots in Fig. 9(A) summarize as initial-selectivity vs. initial-activity plots the results obtained from such comparisons in pulsed flow conditions at T_{rx} 773 to 823 K over 18-OR sample using either O_2 (Plot B) or N_2O (Plot A) as gas-phase oxidant. Various T_{rx} were used to achieve data extending from the high C_4 selectivity/low-conversion regime to the lower-selectivity/higher-conversion regime. In both regimes, higher selectivity resulted from admixed N_2O than from O_2 at comparable activities.

In view of results in (i) above, comparisons such as those in (ii) seemed more likely to reflect differences between the influence of N_2O and of O_2 on post-primary oxidation events as per Scheme 1, than on the primary *n*-butane activation step. Pulsed flow experiments, to determine which of the post primary oxidation processes in Scheme 1 was affected differently by N_2O than by O_2, were made by comparing conversions of butane with N_2O or O_2, and butene with N_2O or O_2. The results in Fig. 10 show how, irrespective of the oxidant, butene reactivity and the diene yield thereof remained unaffected. However, with butane as reactant, the observation of a much diminished diene yield with O_2 relative to that with N_2O pointed to dioxygen being much more efficient in the non-selective oxidation of C_4H_9 to CO_x at 803 K. Analogous pulse-switching experiments between butane-only and butane–N_2O showed no loss of butadiene selectivity at 803 K.

An aspect of foregoing results from pulsed reactant experiments, which makes apparent the inadequacy of any *unmodified* Mars van Krevelen (MVK)-type

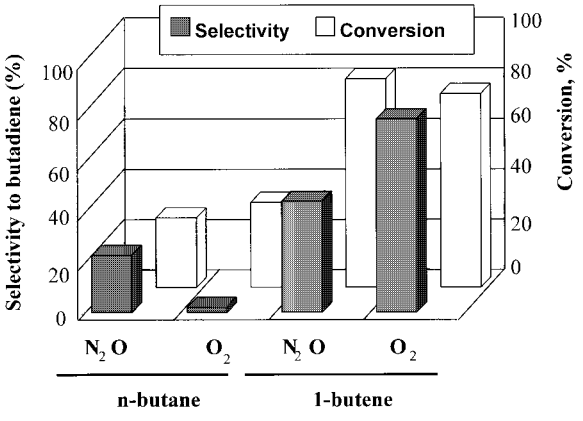

Fig. 10. Selectivity to butadiene and conversion of *n*-butane or 1-butene during the oxidation of *n*-butane or 1-butene at 803 K over the preoxidised 36-OR catalyst, using butane or butene as the C_4 reactant likewise mixed with N_2O or O_2. Experimental conditions as in Fig. 9.

mechanism to account for present results, is the different effects demonstrated for O_2 and N_2O on butadiene selectivity (cf. Fig. 10). Such difference was not to be expected if O_2 and N_2O had simply acted to reoxidize, with equal efficiency, the surface sites which suffered partial reduction in the first step of Scheme 1. On the other hand, and in view of the well-established difference in oxidizing powers of O_2 and N_2O toward organics, similar inadequacy does not attach to the somewhat different post-primary actions envisaged in Scheme 1 for O_2 and N_2O. In this context, differences could be expected in the extent to which O_2 and N_2O promoted non-selective oxidation of organic intermediates to carbon oxides; thus the recognition of this as a mechanistic factor *in addition* to MVK-type reoxidation of surface sites, reduced in the primary step of Scheme 1, is essential. Within Scheme 1, such recognition takes form of much stronger promotion of deep oxidation of C_4H_9 intermediate to carbon oxides by O_2 than by N_2O. Present results from continuous flow catalytic runs, showing higher selectivity to C_4-olefins with N_2O as oxidant than O_2, lend support to operation of this mechanistic factor, in steady-state conditions, since molecular oxygen showed stronger and less selective ODH character than N_2O, possibly via differing reactivities toward C_4H_9 surface intermediates, such as C_4H_9-V^{4+}-OH [38–41].

In conclusion, two variations of the wet-impregnation method have been employed in order to obtain MgO-supported vanadia catalysts with different vanadium-loading and different surface area. MgO and Mg-orthovanadate ($Mg_3V_2O_8$) are the main crystalline phases, although their crystallinities depend on both the preparation method and V-loading of catalysts. On the other hand, tetrahedral V^{5+}-species with different distortion degree are mainly observed, which can be related to Mg-orthovanadate in both amorphous and crystalline phases. These vanadium species also show a different reducibility, the more crystalline phase, the lower reducibility of its vanadium species. Oxygen isotopic-exchange experiments indicate a small activity for homophase isotopic exchange (R_0-type) at 823 K, while an R_2-type is observed at temperatures higher than 1023 K. In addition, it can be concluded, in the reaction conditions used during the ODH of alkanes, that heterophase oxygen isotopic exchange did not occur. However, a high incorporation of oxygen is observed if the catalyst is previously reduced, indicating that reoxidation step is fast.

On the other hand, the catalytic results for the ODH of *n*-butane using O_2 as oxidant indicate that the preparation procedure of catalysts determine the catalytic performance of V–Mg–O catalysts. However, the incorporation of N_2O as oxidant increases the selectivity to butadiene at high butane conversions. This catalytic behavior can be explained on considering that, in these conditions, oxygen species adsorbed on reduced sites can react with olefins favoring deep oxidation reactions, while, in the case of N_2O, a low concentration of adsorbed oxygen on the catalyst surface will favor a low consecutive oxidation of butadiene.

Acknowledgements

Complementary aspects of the cooperative research in two participating laboratories, on which this paper is based, were greatly enhanced by EU funding received within a network funded under contract ERB CH CT 92 0065. J.M. López Nieto, A. Dejoz and M.I. Vazquez also thank the financial support by Comisión Interministerial de Ciencia y Tecnología, CICYT, from Spain (Project MAT 94-0898).

References

[1] H.H. Kung, M.A. Chaar, US Patent 4,772,319 (1988).
[2] M.A. Chaar, D. Patel, M.C. Kung, H.H. Kung, J. Catal. 105 (1987) 483.
[3] A. Corma, J.M. López Nieto, N. Paredes, A. Dejoz, M.I. Vazquez, New Developments in: Selective Oxidation II, Studies in Surface Science and Catalysis, vol. 82, Elsevier, Amsterdam, 1994, p. 113.
[4] T. Blasco, J.M. López Nieto, A. Dejoz, M.I. Vazquez, J. Catal. 157 (1995) 271.
[5] M.A. Chaar, D. Patel, H.H. Kung, J. Catal. 109 (1988) 463.
[6] D. Siew Hew Sam, V. Soenen, J.C. Volta, J. Catal. 123 (1990) 417.
[7] A. Corma, J.M. López Nieto, N. Paredes, J. Catal. 144 (1993) 425.
[8] A. Corma, J.M. López Nieto, N. Paredes, M. Pérez, Y. Shen, H. Cao, S.L. Suib, in: New Developments in Selective Oxidation by Heterogeneous Catalysis, Studies in Surface Science and Catalysis, vol. 72, Elsevier, Amsterdam, 1992, p. 213.
[9] X. Gao, P. Ruiz, Q. Xin, X. Guo, B. Delmon, J. Catal. 148 (1994) 56.
[10] P. Concepción, J.M. López Nieto, J. Pérez-Pariente, J. Molec. Catal. A: Chemical 99 (1995) 173.
[11] J. Hanuza, B. Jezowska-Trzebiatowska, W. Oganowski, J. Molec. Catal. 29 (1985) 109.
[12] J. Kijenski, A. Baiker, M. Glinski, P. Dollenmeier, A. Wokaun, J. Catal. 101 (1986) 1.
[13] V.K. Sharma, A. Wokaum, A. Baiker, J. Phys. Chem. 90 (1986) 2715.
[14] M. Del Arco, M.J. Holgado, V. Rives, J. Mater. Sci. Lett. 6 (1987) 616.
[15] A. Corma, J.M. López Nieto, N. Paredes, Appl. Catal. A: General 104 (1993) 161.
[16] G. Busca, G. Ricchiardi, D. Siew Hew Sam, J.C. Volta, J. Chem Soc. Faraday Trans. 90 (1994) 1161.
[17] O.B. Lapina, A.V. Simakov, V.M. Mastikhin, S.A. Veniaminov, A.A. Shubin, J. Molec. Catal. 50 (1989) 55.
[18] H. Eckert, I.F. Wachs, J. Phys. Chem. 93 (1989) 6796.
[19] M.L. Occelli, R.S. Maxwell, H. Eckert, J. Catal. 137 (1992) 36.
[20] T. Okuhara, K. Inumaru, M. Misono, N. Matsubayashi, H. Shimada, A. Nishijima, Catal. Lett. 20 (1993) 73.
[21] M. Iwamoto, T. Takenaka, K. Matsukami, J. Hirata, S. Kayama, J. Uzumi, Appl. Catal. 16 (1985) 153.
[22] V.A. Shvets, V.B. Kazanski, J. Catal. 25 (1972) 123.
[23] V.K. Sharma, A. Wokaun, A. Baiker, J. Phys. Chem. 90 (1986) 2715.
[24] A.V. Simakov, A.A. Veniaminov, React. Kinet. Catal. Lett. 28 (1985) 67.
[25] V.A. Fenin, V.A. Shvets, V.B. Kazanskii, Kinet. Catal. 16 (1976) 902.
[26] V.A. Kalif, B.V. Rozentuller, E.L. Aptekar, K.N. Spiridonov, O.V. Krylov, Kinet. Catal. 19 (1979) 1001.
[27] Y. Murakami, M. Inomata, K. Mori, T. Ui, K. Suzuki, A. Miyamoto, T. Hattori, Proc. 3th Int. Symp. Scientific Bases for the Preparation of Heterogeneous Catalysts, Lovain-la-Neuve, 1982, paper F-31.
[28] A.A. Rar, A.V. Simakov, S.A. Veniaminov, React. Kinet. Catal. Lett. 39 (1989) 299.
[29] V.A. Fenin, V.A. Shvets, V.B. Kazanskii, Kinet. Catal. 20 (1980) 777.
[30] M.C. Kung, H.H. Kung, J. Catal. 134 (1992) 668.
[31] J.M. López Nieto, A. Dejoz, M.I. Vazquez, Appl. Catal. A: General 132 (1995) 41.
[32] X. Gao, Q. Xin, X. Guo, Appl. Catal. A: General 114 (1994) 197.
[33] F.D. Hardcastle, I.E. Wachs, H. Eckert, D.A. Jefferson, J. Solid State Chem. 90 (1991) 194.
[34] J. Cunningham, E.L. Goold, E.M. Leahy, J. Chem. Soc. Faraday Trans. 75 (1979) 305.
[35] J. Novakova, Catal. Rev.-Sci. Eng. 4 (1970) 78.
[36] J. Cunningham, E.L. Goold, J.L.G. Fierro, J. Chem. Soc. Farad. Trans. 78 (1982) 758.
[37] M. Che, B.N. Shelimov, J.F.J. Kibblewhite, A.J. Tench, Chem. Phys. Lett. 28 (1974) 387.
[38] G. Bellusi, C. Centi, S. Perathoner, F. Trifirò, in: Catalytic Selective Oxidation, A.C.S. Symposium Series, vol. 523, American Chemical Society, Washington, 1993, p. 281.
[39] A. Erdöhelvi, F. Solymosi, J. Catal. 123 (1990) 31.
[40] A. Erdöhelvi, F. Solymosi, J. Catal. 129 (1990) 497.
[41] L. Mendelovici, J.H. Lunsford, J. Catal. 94 (1985) 37.
[42] N.I. Ilchenko, N. Hanke, L.N. Rayevskaya, G.I. Golodets, G. Ohlman, React. Kinet. Catal. Lett. 41 (1990) 147.